PHYSICAL REVIEW B VOLUME 40, NUMBER 7 1 SEPTEMBER 1989

Soliton theory for realistic magnetic domain-wall dynamics

H. How,* R. C. O'Handley, and F. R. Morgenthaler
Massachusetts Institute of Technology, Cambridge, Massachusetts 02139
(Received 20 April 1987; revised manuscript received 9 January 1989)

The dynamics of a 180° ferromagnetic domain wall subject only to uniaxial anisotropy and exchange potentials can be described by the sine-Gordon equation. We extend these treatments to more realistic cases by adding terms due to an external magnetic field, Gilbert damping, and magnetoelastic interaction. The dynamical response of the above added physical couplings, which disturb the soliton's motion as well as modify the soliton's profile, can then be studied in detail via perturbation theory. Results concerning field driving and Gilbert damping are found to coincide with Walker's solution up to the second perturbation order, whereas magnetoelastic coupling modifies the shape of the domain wall in a way which reveals the possibility of a resonant dependence on the wall's traveling velocity.

I. INTRODUCTION

The dynamical behavior of a sine-Gordon soliton in the presence of external perturbations has been discussed in depth by Fogel *et al.*, where they concluded that sine-Gordon solitons in many respects behave as deformable classical particles whose dynamics are governed by Newton's law.[1,2] The dynamics of the interaction of a 180° ferromagnetic domain wall with a planar defect characterized by an abrupt change in both the magnetic anisotropy and exchange energies was considered by Paul where, via solitary wave theory, he obtained the general algebraic expressions for the resonant domain-wall oscillation frequency, the effective wall stiffness, and the coercive force.[3] In this paper, we add perturbations to the original sine-Gordon equation, which describe more realistically the physical couplings to the motion of a 180° ferromagnetic domain wall. This is done by using effective-field theory and is contrasted with the conventional Hamiltonian approach, which starts from a formulation of the exchange and anisotropy potentials in addition to the kinetic energy associated with the spin's precessing motion within the wall.[3,4] Whereas the Hamiltonian approach is difficult to generalize to include any other physical interactions, the effective-field approach lends itself more readily to physical interpretation and is consequently more transparent in its applicability and limitations.[5,6]

Based on effective-field theory, a derivation of the first-order perturbations to the sine-Gordon equation due to an external magnetic field, Gilbert damping, and magnetoelastic interaction is presented in Sec. II. The technique of solving such a perturbed sine-Gordon equation and its physical interpretation can be found in Ref. 1. In Sec. III we examine the perturbation solution of a soliton's motion in the presence of Gilbert damping and a quasistatic field applied in the easy direction. We find that a balance between the field-driven acceleration and Gilbert damping is achieved and the terminal velocity the wall acquires is the same as that derived conventionally.[7,8] It is noted that the perturbation force corresponding to the driving field is different from that considered by Fogel *et al.* in Ref. 1. The driving field considered by Fogel *et al.* is spatially uniform, whereas the true Zeeman torque is nonvanishing only within the domain-wall region. Therefore, the Zeeman perturbation is accentuated at the soliton's center. The uniform or long-range effect of the force suggested by Fogel *et al.* results in an overall shift of the wings of the soliton by an amount proportional to the magnitude of the driving force. This is not the case for a magnetic accelerating field, where the associated perturbation has no first-order effect in changing the domain-wall's magnetization profile. The viscous term used by Fogel *et al.* is coincidentally the same as the Gilbert damping force considered here only if the lowest perturbation order is considered. The perturbation results are found to coincide with Walker's solution[9] up to the second perturbation order, although only the first-order effects of the couplings are attempted in the calculations.

Magnetoelastic coupling to the domain-wall's motion is considered in Sec. IV. It is found that the soliton's profile is slightly modified by this coupling and dynamic strains are induced through the motion of the domain wall. These strains are localized about the domain-wall's center. Moreover, the dynamically induced local strains give rise to a resonant dependence on the wall's velocity such that large strains could be induced if the wall travels with a velocity equal to that of acoustic waves. This effect should be accessible to direct experimental observation. Magnetoelastic coupling is found to not disturb the soliton's motion in first-order perturbation.

II. PERTURBATIONS TO SINE-GORDON EQUATION AND ACOUSTIC-WAVE EQUATIONS

The geometry related to a 180° domain-wall configuration is defined first. Let $\hat{\mathbf{x}}$ be the easy axis with a uniaxial anisotropy K and $\hat{\mathbf{z}}$ be the direction normal to the wall. Assume all the physical boundaries are relaxed

and, hence, all the physical quantities have spatial variations only in the z direction. Gaussian units will be used in this analysis. Magnetization reversal for a single domain-wall soliton is shown in Fig. 1, and the spherical coordinate system used is shown in Fig. 2. Here

$$\mathbf{M}=M_s\hat{\mathbf{u}} ,$$

$$M_x=M_s\sin\theta\cos\phi ,$$

$$M_y=M_s\sin\theta\sin\phi ,$$

$$M_z=M_s\cos\theta ,$$

and M_s is the saturation magnetization. Note that the coordinates used here are different from that used by Walker. In Walker's coordinates the wall is parallel to the xz plane with $\hat{\mathbf{z}}$ being the easy direction. Walker's solution was derived by assuming all the magnetization vectors of a moving domain wall to be restricted to a single azimuthal half-plane with the azimuthal angle depending on the wall's moving velocity. Therefore, in order to more readily compare a perturbed domain-wall solution with Walker's solution, one might wish to adopt Walker's coordinate configuration as long as the sine-Gordon equation is still derivable as the zeroth-order equation in that configuration. However, it turns out not to be the case, although an erroneous derivation has been deduced in Ref. 10.

It is also noted that for a moving domain wall of low velocity the small out-of-plane angle $\eta=\pi/2-\theta$, which measures the departure of the spins within the wall away from the xy plane, is nonzero and is treated as the "smallness number" used in our perturbation scheme. For a moving domain wall it is the out-of-plane magnetization that produces a demagnetizing field which acts back on each individual spin inducing precession motions of the spins in the xy plane. This, in turn, results in a displacement of the wall as a whole in the z direction and hence sustains the wall's traveling motion. Therefore, the demagnetizing field gives the wall an inertial mass.

The equation of motion for magnetization is

$$\frac{\partial\mathbf{M}}{\partial t}=-\gamma\mathbf{M}\times\mathbf{H}_{\rm tot} , \tag{2.1}$$

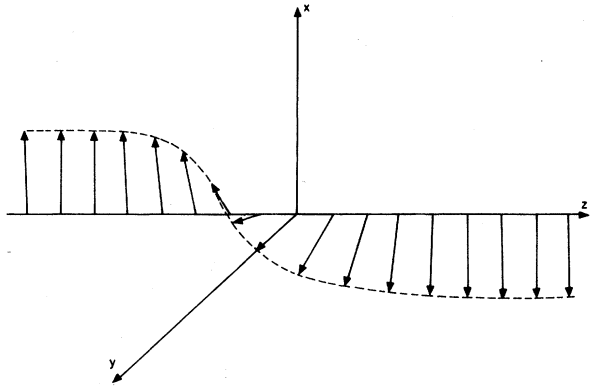

FIG. 1. Magnetization reversal for a 180° domain-wall soliton.

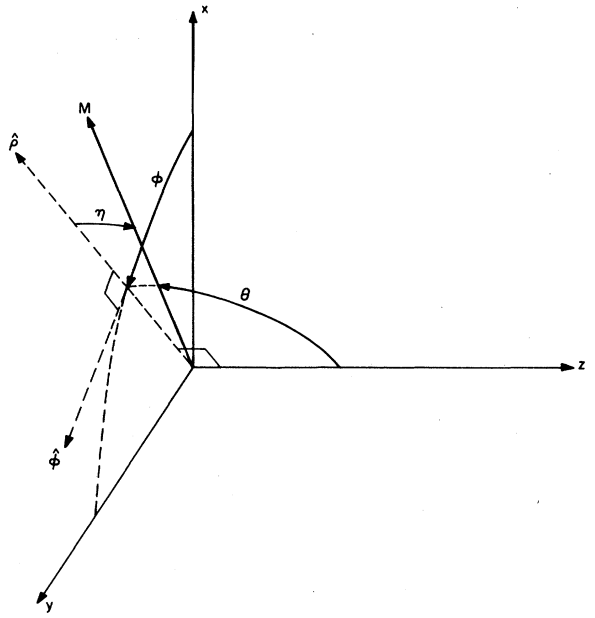

FIG. 2. Coordinate notations: $\hat{\mathbf{x}}$ is the easy direction, ϕ the azimuthal angle of the magnetization, θ the polar angle, and $\eta=\pi/2-\theta$.

where γ is gyromagnetic ratio, and $\mathbf{H}_{\rm tot}$ denotes the total effective field experienced by the spins.[5,6] For a given energy density distribution $w(\mathbf{M},\partial\mathbf{M}/\partial x_i)$, which, in general, depends not only on the magnetization $\mathbf{M}$ but also on the magnetic strains $\partial\mathbf{M}/\partial x_i$, the effective field is

$$(\mathbf{H}_{\rm eff})_i=-\frac{\partial w}{\partial M_i}+\sum_{j=1}^{3}\frac{\partial}{\partial x_j}\frac{\partial w}{\partial(\partial M_i/\partial x_j)} . \tag{2.2}$$

In this analysis we assume the total effective field $\mathbf{H}_{\rm tot}$ to be composed of the following physical components:

$$\mathbf{H}_{\rm tot}=\mathbf{H}_0+\mathbf{H}_d+\mathbf{H}_G+\mathbf{H}_{\rm an}+\mathbf{H}_{\rm ex}+\mathbf{H}_{\rm mag} ,$$

where $\mathbf{H}_0$ is the external field, $\mathbf{H}_d$ the demagnetizing field, $\mathbf{H}_G$ the Gilbert damping field, and $\mathbf{H}_{\rm an}$, $\mathbf{H}_{\rm ex}$, and $\mathbf{H}_{\rm mag}$ are the effective fields associated with anisotropy, exchange, and magnetoelastic interaction, respectively. When expressed in spherical coordinates, Eq. (2.1) takes the form

$$\frac{\partial\theta}{\partial t}=\gamma(\mathbf{H}_{\rm tot})_\phi , \tag{2.3a}$$

$$\sin\theta\frac{\partial\phi}{\partial t}=-\gamma(\mathbf{H}_{\rm tot})_\theta . \tag{2.3b}$$

Let the dc field $\mathbf{H}_0$ be applied along the easy direction

$$\mathbf{H}_0=H_0\hat{\mathbf{x}}$$
$$=H_0(\sin\theta\cos\phi\hat{\mathbf{u}}+\cos\theta\cos\phi\hat{\boldsymbol{\theta}}-\sin\phi\hat{\boldsymbol{\phi}}) . \tag{2.4}$$

In a magnetic substance the demagnetizing field is defined by the two relations

$$\nabla\cdot\mathbf{H}_d=-4\pi\nabla\cdot\mathbf{M}\ ,$$
$$\nabla\times\mathbf{H}_d=0\ .$$

The evaluation of demagnetizing effects for an arbitrary excitation is a fairly complicated problem; but if we assume the magnetization varies only in one direction, the z direction, the demagnetizing field has the form

$$\mathbf{H}_d=-4\pi M_z\hat{\mathbf{z}}$$
$$=-4\pi M_s\cos\theta(\cos\theta\hat{\mathbf{u}}-\sin\theta\hat{\boldsymbol{\theta}})\ . \tag{2.5}$$

The Gilbert damping field is

$$\mathbf{H}_G=\frac{-\lambda}{\gamma M_s}\frac{\partial\mathbf{M}}{\partial t}$$
$$=-\frac{\lambda}{\gamma}\left[\frac{\partial\theta}{\partial t}\hat{\boldsymbol{\theta}}+\sin\theta\frac{\partial\phi}{\partial t}\hat{\boldsymbol{\phi}}\right]\ , \tag{2.6}$$

where λ denotes the Gilbert damping constant. The uniaxial anisotropy field is

$$\mathbf{H}_{\rm an}=(2K/M_s^2)M_x\hat{\mathbf{x}}$$
$$=(2K/M_s)\sin\theta\cos\phi(\sin\theta\cos\phi\hat{\mathbf{u}}$$
$$+\cos\theta\cos\phi\hat{\boldsymbol{\theta}}-\sin\phi\hat{\boldsymbol{\phi}})\ , \tag{2.7}$$

and the exchange field is

$$\mathbf{H}_{\rm ex}=\frac{2A}{M_s^2}\frac{\partial^2\mathbf{M}}{\partial z^2}$$
$$=\frac{2A}{M_s}\left\{-\left[\left[\frac{\partial\theta}{\partial z}\right]^2+\sin^2\theta\left[\frac{\partial\phi}{\partial z}\right]^2\right]\hat{\mathbf{u}}\right.$$
$$+\left[\frac{\partial^2\theta}{\partial z^2}-\sin\theta\cos\theta\left[\frac{\partial\phi}{\partial z}\right]^2\right]\hat{\boldsymbol{\theta}}$$
$$\left.+\left[\sin\theta\frac{\partial^2\phi}{\partial z^2}+2\cos\theta\frac{\partial\theta}{\partial z}\frac{\partial\phi}{\partial z}\right]\hat{\boldsymbol{\phi}}\right\}\ . \tag{2.8}$$

Here K is the anisotropy constant and A is the exchange stiffness. The magnetoelastic energy density is[11]

$$w_{\rm mag}=b_1(\alpha_x^2\epsilon_{xx}+\alpha_y^2\epsilon_{yy}+\alpha_z^2\epsilon_{zz})$$
$$+2b_2(\alpha_x\alpha_y\epsilon_{xy}+\alpha_y\alpha_z\epsilon_{yz}+\alpha_z\alpha_x\epsilon_{zx})$$
$$=b_1\alpha_z^2\frac{\partial R_z}{\partial z}+b_2\left[\alpha_x\alpha_z\frac{\partial R_x}{\partial z}+\alpha_y\alpha_z\frac{\partial R_y}{\partial z}\right]\ , \tag{2.9}$$

where b_1 and b_2 are the magnetoelastic constants, α_i's are the direction cosines of the magnetization M, R_i's are the displacement fields, and ϵ_{ij}'s are the strain fields defined by

$$\epsilon_{ij}=\frac{1}{2}\left[\frac{\partial R_i}{\partial x_j}+\frac{\partial R_j}{\partial x_i}\right]\ .$$

Note that ϵ_{xx}, ϵ_{xy}, and ϵ_{yy} vanish in the present one-dimensional geometry and $\epsilon_{xz}=\frac{1}{2}(\partial R_x/\partial z)$, $\epsilon_{yz}=\frac{1}{2}(\partial R_y/\partial z)$, and $\epsilon_{zz}=(\partial R_z/\partial z)$. In this analysis we consider only the infinitesimal strains. For a discussion of the finite strains, see Ref. 12. The effective field associated with the above magnetoelastic energy density is, according to Eq. (2.2),

$$H_{\rm mag}=\frac{-1}{M_s^2}\left\{b_2M_z\left[\frac{\partial R_x}{\partial z}\hat{\mathbf{x}}+\frac{\partial R_y}{\partial z}\hat{\mathbf{y}}\right]+\left[2b_1M_z\frac{\partial R_z}{\partial z}+b_2\left[M_x\frac{\partial R_x}{\partial z}+M_y\frac{\partial R_y}{\partial z}\right]\right]\hat{\mathbf{z}}\right\}$$
$$=\frac{-1}{M_s}\left\{2\cos\theta\left[b_1\cos\theta\frac{\partial R_z}{\partial z}+b_2\sin\theta\left[\cos\phi\frac{\partial R_x}{\partial z}+\sin\phi\frac{\partial R_y}{\partial z}\right]\right]\hat{\mathbf{u}}\right.$$
$$\left.+\left[-b_1\sin2\theta\frac{\partial R_z}{\partial z}+b_2\cos2\theta\left[\cos\phi\frac{\partial R_x}{\partial z}+\sin\phi\frac{\partial R_y}{\partial z}\right]\right]\hat{\boldsymbol{\theta}}-b_2\cos\theta\left[\sin\phi\frac{\partial R_x}{\partial z}-\cos\phi\frac{\partial R_y}{\partial z}\right]\hat{\boldsymbol{\phi}}\right\}\ . \tag{2.10}$$

For $\eta=\pi/2-\theta\ll1$ we expand all the above expressions for the effective fields to the first order in η and sum them up. The results are

$$(\mathbf{H}_{\rm tot})_\phi\approx-H_0\sin\phi-\frac{2K}{M_s}\sin\phi\cos\phi+\frac{2A}{M_s}\frac{\partial^2\phi}{\partial z^2}-\frac{\lambda}{\gamma}\frac{\partial\phi}{\partial t}+\frac{b_2}{M_s}\left[\sin\phi\frac{\partial R_x}{\partial z}-\cos\phi\frac{\partial R_y}{\partial z}\right]\eta\ , \tag{2.11a}$$

$$(\mathbf{H}_{\rm tot})_\theta\approx H_0\cos\phi\,\eta+4\pi M_s\eta+\frac{2K}{M_s}\cos^2\phi\,\eta-\frac{2A}{M_s}\left[\frac{\partial^2\eta}{\partial z^2}+\eta\left[\frac{\partial\phi}{\partial z}\right]^2\right]$$
$$+\frac{\lambda}{\gamma}\frac{\partial\eta}{\partial t}+\frac{b_2}{M_s}\left[\cos\phi\frac{\partial R_x}{\partial z}+\sin\phi\frac{\partial R_y}{\partial z}\right]+\frac{2b_1}{M_s}\frac{\partial R_z}{\partial z}\eta\ . \tag{2.11b}$$

In order to derive the coupled acoustic wave equations, we apply the Lagrangian formalism to the material's deformation. Under the assumption of elastic isotropy, the Lagrangian density associated with elastic deformation in the present geometry is[11]

$$L_{\rm el}=\frac{\rho}{2}\left[\left[\frac{\partial R_x}{\partial t}\right]^2+\left[\frac{\partial R_y}{\partial t}\right]^2+\left[\frac{\partial R_z}{\partial t}\right]^2\right]-\mu\sum_{i,j}^{3}\epsilon_{ij}^2-\frac{\lambda_L}{2}\left[\sum_{i}^{3}\epsilon_{ii}\right]^2-w_{\rm mag}$$
$$=\frac{\rho}{2}\left[\left[\frac{\partial R_x}{\partial t}\right]^2+\left[\frac{\partial R_y}{\partial t}\right]^2+\left[\frac{\partial R_z}{\partial t}\right]^2\right]-\frac{C_{11}}{2}\left[\frac{\partial R_z}{\partial z}\right]^2-\frac{C_{44}}{2}\left[\left[\frac{\partial R_x}{\partial z}\right]^2+\left[\frac{\partial R_y}{\partial z}\right]^2\right]$$
$$-b_1\alpha_z^2\frac{\partial R_z}{\partial z}-b_2\left[\alpha_x\alpha_z\frac{\partial R_x}{\partial z}+\alpha_y\alpha_z\frac{\partial R_y}{\partial z}\right], \tag{2.12}$$

where ρ is the mass density, μ the bulk modulus, λ_L the Lame constant, and C_{12} $(=\lambda_L)$, C_{44} $(=\mu)$, and C_{11} $(=C_{12}+2C_{44})$ are the elastic constants. Substitution of Eq. (2.12) into the Lagrangian equation of motion

$$\frac{\partial L_{\rm el}}{\partial R_i}-\frac{\partial}{\partial t}\left[\frac{\partial L_{\rm el}}{\partial(\partial R_i/\partial t)}\right]-\frac{\partial}{\partial z}\left[\frac{\partial L_{\rm el}}{\partial(\partial R_i/\partial z)}\right]=0 \tag{2.13}$$

gives the following magnetoelastically coupled acoustic-wave equations:

$$\rho\frac{\partial^2 R_x}{\partial t^2}-C_{44}\frac{\partial^2 R_x}{\partial z^2}=b_2\frac{\partial}{\partial z}(\eta\cos\phi), \tag{2.14a}$$

$$\rho\frac{\partial^2 R_y}{\partial t^2}-C_{44}\frac{\partial^2 R_y}{\partial z^2}=b_2\frac{\partial}{\partial z}(\eta\sin\phi), \tag{2.14b}$$

$$\rho\frac{\partial^2 R_z}{\partial t^2}-C_{11}\frac{\partial^2 R_z}{\partial z^2}=2b_1\eta\frac{\partial\eta}{\partial z}. \tag{2.14c}$$

The above equations are valid only in the lowest order of η.

To be specific, we adopt the following parameters for the magnetic material:

$$\gamma=2\times10^7\ {\rm Oe}^{-1}\,{\rm s}^{-1},$$
$$K=3\times10^4\ {\rm erg\,cm}^{-3},$$
$$A=10^{-6}\ {\rm erg\,cm}^{-1},$$
$$4\pi M_s=10^4\ {\rm G},$$
$$\rho=8\ {\rm g\,cm}^{-3},$$
$$C_{44}=2C_{11}=2\times10^{12}\ {\rm erg\,cm}^{-3},$$
$$b_1=b_2=10^8\ {\rm erg\,cm}^{-3}.$$

The magnetic field is chosen to be 10 Oe and the intrinsic spin-relaxation time $\tau=10^{-8}$ s. This implies the Gilbert damping constant

$$\lambda=(4\pi M_s\gamma\tau)^{-1}=10^{-3}.$$

Dimensionless variables and parameters are now defined. Let space coordinate z be normalized with respect to the wall thickness,

$$\delta=(A/K)^{1/2}=5\times10^{-6}\ {\rm cm}$$

and the time coordinate be normalized with respect to the inverse of the natural frequency,

$$\omega_0^{-1}=(8\pi K\gamma^2)^{-1/2}=5\times10^{-11}\ {\rm s}.$$

The transverse sound velocity,

$$c_t=(C_{44}/\rho)^{1/2}=3\times10^5\ {\rm cm/s},$$

and longitudinal sound velocity,

$$c_l=(C_{11}/\rho)^{1/2}=5\times10^5\ {\rm cm/s},$$

are normalized with respect to the (virtual) magnon's velocity, $c_0=\delta\omega_0=10^5$ cm/s. The resultant dimensionless transverse and longitudinal sound velocities are, respectively, $\beta_t=c_t/c_0=3$ and $\beta_l=c_l/c_0=5$. The strains are normalized with respect to

$$S=(K/\rho c_0^2)^{1/2}=6\times10^{-4}.$$

Perturbation parameters are defined by

$$\nu_H^3=H_0/4\pi M_s\approx10^{-3},$$
$$\nu_G^3=\lambda(8\pi K)^{1/2}/4\pi M_s\approx10^{-4},$$
$$\nu_K=(4\pi K)^{1/2}/4\pi M_s\approx10^{-1},$$
$$\nu_{b1}=(4\pi Sb_1)^{1/2}/4\pi M_s\approx10^{-1},$$
$$\nu_{b2}=(4\pi Sb_2)^{1/2}/4\pi M_s\approx10^{-1}.$$

Perturbations considered in this paper are confined to the regime where all the following parameters are of the same order:

$$\eta\approx\nu_K\approx\nu_H\approx\nu_G\approx\nu_{b1}\approx\nu_{b2}\approx10^{-1}.$$

In terms of the dimensionless parameters Eqs. (2.14a)–(2.14c) can be rewritten as

$$\frac{\partial^2 R_x}{\partial t^2}-\beta_t^2\frac{\partial^2 R_x}{\partial z^2}=\left[\frac{\nu_{b2}}{\nu_K}\right]^2\frac{\partial}{\partial z}(\eta\cos\phi), \tag{2.15a}$$

$$\frac{\partial^2 R_y}{\partial t^2}-\beta_t^2\frac{\partial^2 R_y}{\partial z^2}=\left[\frac{\nu_{b2}}{\nu_K}\right]^2\frac{\partial}{\partial z}(\eta\sin\phi), \tag{2.15b}$$

$$\frac{\partial^2 R_z}{\partial t^2}-\beta_l^2\frac{\partial^2 R_z}{\partial z^2}=\left[\frac{\nu_{b1}}{\nu_K}\right]^2\frac{\partial}{\partial z}(\eta^2). \tag{2.15c}$$

Substituting Eqs. (2.11a) and (2.11b) into Eqs. (2.3a) and (2.3b) and using dimensionless parameters, one obtains

$$-\sqrt{2}\nu_K\frac{\partial\eta}{\partial t}=2\nu_K^2\left[\frac{\partial^2\phi}{\partial z^2}-\sin\phi\cos\phi\right]-\nu_H^3\sin\phi-\nu_G^3\frac{\partial\phi}{\partial t}+\nu_{b2}^2\eta\left[\sin\phi\frac{\partial R_x}{\partial z}-\cos\phi\frac{\partial R_y}{\partial z}\right], \quad (2.16a)$$

$$-\sqrt{2}\nu_K\frac{\partial\phi}{\partial t}=\eta+2\nu_K^2\left[\eta\cos^2\phi-\frac{\partial^2\eta}{\partial z^2}-\eta\left[\frac{\partial\phi}{\partial z}\right]^2\right]+\nu_H^3\eta\cos\phi+\nu_G^3\frac{\partial\eta}{\partial t}+2\nu_{b1}^2\eta\frac{\partial R_z}{\partial z}+\nu_{b2}^2\left[\cos\phi\frac{\partial R_x}{\partial z}+\sin\phi\frac{\partial R_y}{\partial z}\right]. \quad (2.16b)$$

Up to the second perturbation order, Eq. (2.16b) becomes

$$\eta\approx-\frac{\sqrt{2}}{2}\nu_K\frac{\partial\psi}{\partial t}-\nu_{b2}^2\left[\cos\frac{\psi}{2}\frac{\partial R_x}{\partial z}+\sin\frac{\psi}{2}\frac{\partial R_y}{\partial z}\right]+O(\eta^3). \quad (2.17)$$

Here ψ is defined to be twice the azimuthal angle of the magnetization away from the easy direction. When η has been eliminated by using Eq. (2.17), differential equations (2.15a)–(2.15c), and (2.16a) become, up to the lowest perturbation order, respectively,

$$\frac{\partial^2 R_x}{\partial t^2}-\beta_t^2\frac{\partial^2 R_x}{\partial z^2}=B\frac{\partial^2}{\partial z\partial t}\sin\frac{\psi}{2}+O(\eta^2), \quad (2.18a)$$

$$\frac{\partial^2 R_y}{\partial t^2}-\beta_t^2\frac{\partial^2 R_y}{\partial z^2}=-B\frac{\partial^2}{\partial z\partial t}\cos\frac{\psi}{2}+O(\eta^2), \quad (2.18b)$$

$$\frac{\partial^2 R_z}{\partial t^2}-\beta_l^2\frac{\partial^2 R_z}{\partial z^2}=\nu_{b1}^2\frac{\partial}{\partial z}\left[\frac{\partial\psi}{\partial t}\right]^2+O(\eta^3), \quad (2.18c)$$

$$\frac{\partial^2\psi}{\partial t^2}+\sin\psi-\frac{\partial^2\psi}{\partial z^2}=-f\sin\frac{\psi}{2}-\Gamma\frac{\partial\psi}{\partial t}+B\left[\cos\frac{\psi}{2}\frac{\partial^2 R_x}{\partial z\partial t}+\sin\frac{\psi}{2}\frac{\partial^2 R_y}{\partial z\partial t}\right]+O(\eta^2), \quad (2.18d)$$

where

$$f=\nu_H^3/\nu_K^2=H_0M_s/K\approx10^{-1},$$
$$\Gamma=\nu_G^3/(2\nu_K^2)=\lambda M_s(2\pi/K)^{1/2}\approx10^{-2},$$
$$B=\sqrt{2}\nu_{b2}^2/\nu_K=b_2(4\pi M_s\gamma)^{-1}(A\rho)^{-1/2}\approx10^{-1},$$

are three newly defined parameters which characterize, respectively, the coupling strength of the Zeeman driving field, the Gilbert damping, and the magnetoelastic interaction. All of them are of the same order as η.

Perturbation theory associated with the sine-Gordon solitons can be found in Ref. 1 and is only briefly summarized here. The sine-Gordon equation

$$\frac{\partial^2\psi}{\partial t^2}-\frac{\partial^2\psi}{\partial z^2}+\sin\psi=0 \quad (2.19)$$

has single-particle soliton (+) and antisoliton (−) solutions

$$\psi_\pm^\beta(z,t)=4\tan^{-1}\{\exp[\pm\gamma'(z-\beta t)]\} \quad (2.20)$$

with $\gamma'=(1-\beta^2)^{-1/2}$ and β being the normalized velocity of the particle. Infinitesimal excitations of Eq. (2.19) form a continuous spectrum characterized by the dispersion relation

$$\omega_k^2=1+k^2. \quad (2.21)$$

In a magnetic medium we call the above excitations virtual magnons to distinguish them from the real magnons. Virtual magnons are merely mathematical entities because they do not couple to electromagnetic waves.

Let the perturbation term(s) denoted as $\underline{R}$ appear on the left-hand side of Eq. (2.19). $\underline{R}$ has the general dependence $\underline{R}(\psi;\partial/\partial t,\partial/\partial z,t,z)$. When transformed to the (anti)soliton's rest frame under a Lorentz boost L^β, $\underline{R}$ takes the form

$$L^\beta(\underline{R})=\underline{R}\left[\psi;\gamma'\left[\frac{\partial}{\partial t}-\beta\frac{\partial}{\partial z}\right],\gamma'\left[\frac{\partial}{\partial z}-\beta\frac{\partial}{\partial t}\right],\gamma'(t+\beta z),\gamma'(z+\beta t)\right]. \quad (2.22)$$

In the presence of perturbation(s) and in the (anti)soliton's rest frame, the (anti)soliton solution now has the form

$$\psi(z,t)=\psi_\pm^0(z)+\zeta(z,t), \quad (2.23)$$

where $\psi_\pm^0(z)$ is given by Eq. (2.20) with $\beta=0$ and $|\zeta(z,t)|\ll1$. $\zeta(z,t)$ is expanded in terms of the scattered virtual magnon spectrum as[1]

$$\zeta(z,t)=\tfrac{1}{8}u_b(t)f_b(z)+\int_{-\infty}^{\infty}dk\,u_k(t)f_k(z), \quad (2.24)$$

where $f_b(z)$ and $f_k(z)$ are, respectively, the bound (Goldstone) state and the scattered continuum states of the virtual magnons in the presence of the (anti)soliton, and

$$f_b(z)=2\,\mathrm{sech}(z), \quad (2.25a)$$

$$f_k(z)=(2\pi)^{-1/2}\omega_k^{-1}[k+i\tanh(z)]\exp(ikz). \quad (2.25b)$$

Here ω_k and k still satisfy the dispersion relation Eq. (2.21). Therefore, the (anti)soliton's profile is modified by an amount, say, $\zeta_c(z,t)$, and its center of mass, with locus

defined as $z_c(t)=\mp u_b(t)/8$, is subject to an effective force $F(t)$ as

$$\frac{d^2z_c}{dt^2}=F(t) .$$

From Ref. 1 one can write

$$F(t)=\pm\tfrac{1}{8}\int_{-\infty}^{\infty} dz\, f_b(z)L^{\beta}(\underline{R}) , \tag{2.26a}$$

$$\zeta_c(z,t)=\int_{-\infty}^{\infty} dk\, u_k(t)f_k(z) , \tag{2.26b}$$

with $u_k(t)$ satisfying the following differential equation:

$$\frac{d^2u_k}{dt^2}+\omega_k^2u_k+\int_{-\infty}^{\infty} dz\, f_k^*(z)L^{\beta}(\underline{R})=0 . \tag{2.26c}$$

Note that the present perturbation theory only deals with how the added perturbations can influence the soliton's motion and the soliton's (axial) profile but not the domain wall's planar geometry. It is pointed out by Winter[13] that the wall excitations with sinusoidal variations in its geometric shape contribute most to nuclear resonance. Slonczewski[14] suggests that at intermediate applied fields a spatially corrugated wall might be a stable wall configuration when both Walker's solution (low-field configuration) and the oscillating wall solution (high-field configuration) become either unstable or nonexisting. These nonplanar wall excitations reflect the limitations of the present perturbation theory. However, due to its elegant mathematical representations, soliton perturbation theory can still be very valuable in formulating domain-wall dynamics if the restriction of the problem to one dimension does not preclude treatment of the effect of interest.

III. ACCELERATION AND DAMPING OF A DOMAIN-WALL SOLITON

Let the domain-wall soliton be driven by a quasistatic field applied in the easy direction and subject to Gilbert damping. The corresponding perturbations, according to Eq. (2.18d), are

$$\underline{R}=f\sin\frac{\psi}{2}+\Gamma\frac{\partial\psi}{\partial t} . \tag{3.1}$$

After Lorentz transformation to the soliton's rest frame Eq. (3.1) becomes, according to Eq. (2.22),

$$\begin{aligned} L^{\beta}(\underline{R})&=f\sin\frac{\psi}{2}+\Gamma\gamma'\left[\frac{\partial\psi}{\partial t}-\beta\frac{\partial\psi}{\partial z}\right] \\ &\approx f\sin\frac{\psi_{\pm}^0}{2}+\Gamma\gamma'\left[\frac{\partial\xi}{\partial t}-\beta\frac{d\psi_{\pm}^0}{dz}\right] \\ &=f\,\mathrm{sech}(z)+\Gamma\gamma'\left[\frac{\partial\xi}{\partial t}\mp 2\beta\,\mathrm{sech}(z)\right] , \end{aligned} \tag{3.2}$$

where expression (2.23) has been used for $\psi(z,t)$. Note that in deriving Eq. (3.2) the velocity β, which is proportional to the out-of-plane angle η, has been treated as a small number. From Eqs. (2.24), (2.26a), and (2.26c) one obtains

$$\frac{d^2u_k}{dt^2}+\Gamma\gamma'\frac{du_k}{dt}+\omega_k^2u_k=0 , \tag{3.3}$$

$$\frac{d^2z_c}{dt^2}=\pm\frac{f}{2}-\Gamma\gamma'\left[\frac{dz_c}{dt}+\beta\right] . \tag{3.4}$$

In deriving Eq. (3.4) the translational meaning of the Goldstone mode has been used. For $t\gg\Gamma\gamma'$ the transient part of the solutions to Eqs. (3.3) and (3.4) decays away and the steady-state solutions are

$$(u_k)_{\infty}=0 , \tag{3.5}$$

$$\left[\frac{dz_c}{dt}\right]_{\infty}=\pm\frac{f}{2\Gamma\gamma'}-\beta . \tag{3.6}$$

From Eqs. (2.26) and (3.5) we conclude that to first order the Zeeman and Gilbert perturbations have no effect at all in changing the domain-wall's shape. This situation differs from that in Ref. 1 where an overall shift of the soliton wings occurs as a consequence of an unusual long-range driving force. When Walker's solution is written in terms of the spherical coordinates shown in Fig. 2, a comparison of it to the soliton solution, Eq. (2.20), shows that soliton solution coincides with Walker's solution up to the second perturbation order.

The solution for $(dz_c/dt)_{\infty}$ derived in Eq. (3.6) represents the terminal velocity the wall acquires when observed in a coordinate frame moving initially with the wall. When viewed in the laboratory frame, the above velocity becomes

$$\beta^*=\left[\frac{dz_c}{dt}\right]_{\infty,\mathrm{lab}}=\pm\frac{f}{2\Gamma\gamma'} . \tag{3.7}$$

When expressed in terms of ordinary space and time units, Eq. (3.7) becomes

$$v=\pm\mu_0H_0(1+\mu_0^2H_0^2/c_0^2)^{-1/2} , \tag{3.8}$$

where

$$\mu_0=\frac{fc_0}{2\Gamma H_0}=\frac{\gamma}{\lambda}\left[\frac{A}{K}\right]^{1/2} \tag{3.9}$$

is defined to be the initial mobility of the wall in an applied field. Equation (3.8) is plotted in Fig. 3. In the initial low-field regime $\gamma'\approx 1$ and

$$v=\pm\mu_0H_0=\pm\frac{\gamma H_0}{\lambda}\left[\frac{A}{K}\right]^{1/2} . \tag{3.10}$$

This linear relationship, Eq. (3.10), was first derived by Kittel by considering energy conservation between the applied driving force and the Gilbert damping.[7,15] Consideration of higher-order effects of the present perturbations can be carried out in a straightforward manner. However, the calculations will become quite involved as the virtual magnon modes begin to couple among each other.

The terminal velocity of the wall derived via perturbation theory is compared to that predicted by Walker's solution. As shown in Fig. 4 for various ν_K values,

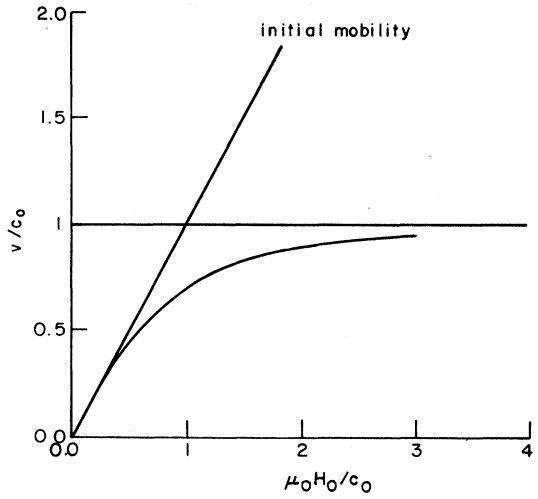

FIG. 3. Domain-wall velocity v vs driving field strength H_0. For large values of H_0 v approaches a constant value c_0 which characterizes the velocity of the massless virtual magnons.

curves labeled (a) represent the linear relationship of Eq. (3.10), curves (b) show the results of Eq. (3.8), and curves (c) are the velocities from Walker's analytic solution. Dashed lines denote velocity bounds beyond which Walker's solution does not exist. Actually, prior to the breakdown of those velocity bounds, Walker's solution can be unstable as long as the differential mobility of the wall becomes negative, as shown in Fig. 4 for the cases

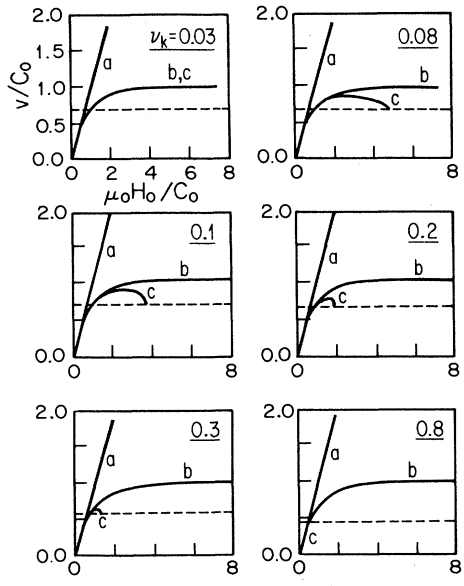

FIG. 4. Comparison of the Kittel's initial linear relationship (curves a), soliton's relativistic results (curves b), and Walker's analytic solutions (curves c) for different ν_K values. ν_K $[=(4\pi K)^{1/2}/4\pi M_s]$ represents the relative strength of the anisotropy field to the saturation magnetization.

$\nu_K \geq 0.08$. The perturbation theory also yields a limiting velocity c_0 for the domain wall's motion, but its nature lies entirely in the relativistic nature of the original sine-Gordon equation, Eq. (2.19). From the derivation of the perturbed sine-Gordon equation, Eqs. (2.16)–(2.18), we see that the behavior of a ferromagnetic domain wall can resemble that of a real soliton only in the limit of high magnetization ($\nu_K \ll 1$) and low demagnetization ($\eta,\beta \ll 1$). This is also revealed in Fig. 4 where the perturbation results approximate Walker's solution only when the wall is moving in the initial regime of low velocity or for the cases that ν_K is small.

There exists another perturbation scheme due to Slonczewski[14] which deals with the limit of low magnetization ($\nu_K \gg 1$). These two perturbation schemes, soliton perturbation and Sloczewski's, are complementary to each other. As noted in the literature, a sine-Gordon soliton is always (linearly) stable against disturbance since ω_k^2 in Eq. (2.21) is always non-negative.[1,16,17] A stability analysis in Slonczewski's scheme ($\nu_K \gg 1$) shows[14] that at intermediate field strength Walker's solution (low-field configuration) and the oscillating wall solution (high-field configuration) could both be unstable. When this happens, as suggested by Slonczewski, the stable configuration might be a spatially corrugated wall. The correspondence of the soliton solution and the uniform mode of Slonczewski's solution to Walker's solution in the low ν_K and high ν_K limits, respectively, provides support for the validity of Walker's solution. As noted by Dillon[9] in presenting Walker's solution, the assumption leading Walker's solution that restricts the whole magnetization reversal process to a single azimuthal half-plane cannot be physically justified. We also mention here that the dynamic response of the breather solutions for the soliton perturbation scheme may merit further attention. This is because the breather solutions exhibit internal oscillations and may play a role related to the oscillating wall solution modes in the high-field configuration of Slonczewski's perturbation scheme.

IV. MAGNETOELASTIC COUPLING AND DYNAMIC STRAINS

Elastic strains exist locally about a static domain wall when the magnetoelastic coupling is nonzero. This is due simply to the spatial variation of magnetization direction within the wall. Similarly, time-dependent magnetoelastic strains could be induced dynamically through the motion of the domain wall as expressed in Eqs. (2.18a)–(2.18c). Since the longitudinal displacement field R_z does not couple in first order to the domain wall's motion in Eq. (2.18d) and the induction of R_z through magnetoelastic interaction b_1 occurs only in second order in Eq. (2.18c), we shall omit further discussion of R_z in the following analysis. The lowest-order expressions for the transverse displacement fields R_x and R_y are obtained by replacing ψ in Eqs. (2.18a) and (2.18b) with $\psi_{\pm}^{\beta}$ given by Eq. (2.20). The resultant acoustic-wave equations then admit the following set of solutions which move with the soliton:

$$R_x(z,t)=-\frac{B\beta}{\beta^2-\beta_t^2}\text{sech}[\gamma'(z-\beta t)]\ , \tag{4.1a}$$

$$R_y(z,t)=\mp\frac{B\beta}{\beta^2-\beta_t^2}\tanh[\gamma'(z-\beta t)]\ . \tag{4.1b}$$

These solutions can be verified by directly substituting them back into Eqs. (2.18a) and (2.18b). They actually represent the unique set of solutions which permits only localized strains. The associated strain fields can be obtained by differentiating Eqs. (4.1a) and (4.1b) with respect to z and the results are

$$\epsilon_{xz}(z,t)=\frac{B}{2}\frac{\gamma'\beta}{\beta^2-\beta_t^2}\left[\frac{K}{\rho c_0^2}\right]^{1/2} \times\text{sech}\left[\frac{\gamma'}{\delta}(z-vt)\right]\tanh\left[\frac{\gamma'}{\delta}(z-vt)\right]\ , \tag{4.2a}$$

$$\epsilon_{yz}(z,t)=\mp\frac{B}{2}\frac{\gamma'\beta}{\beta^2-\beta_t^2}\left[\frac{K}{\rho c_0^2}\right]^{1/2} \times\text{sech}^2\left[\frac{\gamma'}{\delta}(z-vt)\right]\ . \tag{4.2b}$$

Here ϵ_{xz} and ϵ_{yz} are expressed in terms of ordinary space and time units. Profiles of magnetization and dynamic strain components are shown in Fig. 5. Note that the dynamic strains are localized in the vicinity of the domain wall. For the quasistatic case with $\beta=0.1$, the dynamically induced strains are of magnitude equal to 4×10^{-7}, which is about 10^{-2} times the static strains caused by macroscopic magnetostriction. However, for a magnetic material whose transverse sound velocity c_t is less than the virtual magnon's velocity c_0, these dynamic strains could be anomalously enlarged as long as the wall is moving with a velocity approaching c_t. This is because only when the wall moves with a velocity close to that of acoustic waves can the wall carry significant amount of elastic deformation with it.

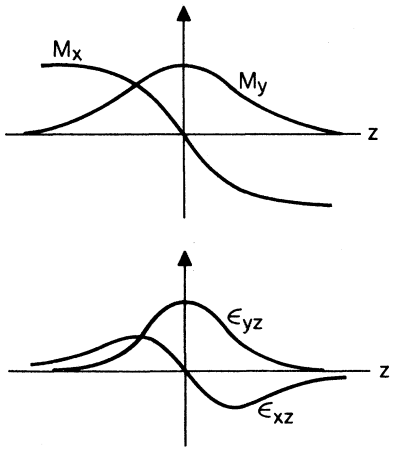

FIG. 5. Magnetization components M_x and M_y and the magnetoelastically induced transverse strains ϵ_{xz} and ϵ_{yz}.

One important implication of the above-mentioned domain-wall velocity resonance might be the following. Under certain circumstances magnetic domain walls may penetrate deeper or with greater velocity into a material than would be dictated by classical eddy current (skin depth) considerations. This effect is contrasted with the phenomenon of "anomalous microwave transmission" proposed by Heinrich[18] and Alexandrakis.[19] While anomalous microwave transmission occurs by coupling of small amplitude spin waves and elastic waves, our model suggests the possibility of anomalous domain-wall motion by coupling to elastic waves under certain conditions through the same magnetoelastic interaction. A detailed analysis of this resonant domain-wall behavior demands a full consideration of the whole set of equations (2.14a), (2.14b), (2.16a), and (2.16b), since the present perturbation scheme breaks down at resonance and the sine-Gordon equation (2.19) can no longer describe satisfactorily the zeroth-order domain-wall dynamics. This requires numerical calculations and merits further investigation.

The lowest-order perturbation associated with magnetoelastic interaction appearing in the sine-Gordon equation is, according to Eq. (2.18d),

$$\underline{R}=-B\left[\cos\frac{\psi}{2}\frac{\partial^2 R_x}{\partial z\partial t}+\sin\frac{\psi}{2}\frac{\partial^2 R_y}{\partial z\partial t}\right]\ . \tag{4.3}$$

Substituting Eqs. (4.1a) and (4.1b) into Eq. (4.3) and then performing a Lorentz transformation to the soliton's rest frame, one obtains, up to the second perturbation order,

$$L^{\beta}(\underline{R})\approx -B\left[\frac{B\beta}{\beta^2-\beta_t^2}\right](-\beta\gamma'^2) \times\left[-\cos\frac{\psi_{\pm}^0}{2}\frac{d^2\text{sech}(z)}{dz^2}\mp\sin\frac{\psi_{\pm}^0}{2}\frac{d^2\tanh(z)}{dz^2}\right] =\pm\frac{B^2\beta^2\gamma'^2}{\beta^2-\beta_t^2}\tanh(z)\,\text{sech}(z)\ . \tag{4.4}$$

From Eqs. (2.25a) and (2.25b) one performs the following integrations:

$$\int_{-\infty}^{\infty}dz\,f_b(z)L^{\beta}(\underline{R})=0\ , \tag{4.5a}$$

$$\int_{-\infty}^{\infty}dz\,f_k^*(z)L^{\beta}(\underline{R})=\mp\frac{i}{4}\sqrt{2\pi}\frac{B^2\beta^2\gamma'^2}{\beta^2-\beta_t^2}\omega_k\,\text{sech}\frac{k\pi}{2}\ . \tag{4.5b}$$

Note that Eq. (4.5a) can be obtained by considering the parities of $f_b(z)$ (even) and $L^{\beta}(\underline{R})$ (odd). The effective force defined in Eq. (2.26a) associated with the present perturbations is consequently zero. This means that the soliton's motion is not disturbed up to the second perturbation order by the dynamically induced strain fields shown in Eqs. (4.2a) and (4.2b). This is true only when the strains are small and are not resonantly enhanced. From Eq. (2.27) the steady-state solution of the decomposition amplitude $u_k(t)$ is

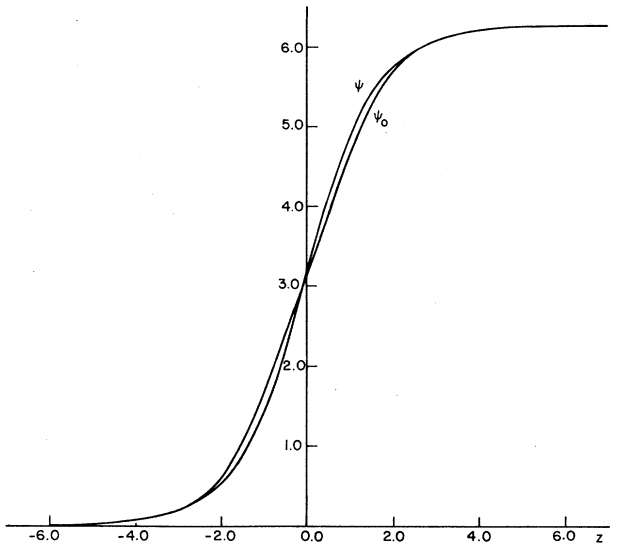

FIG. 6. Modification of domain-wall profiles due to magnetoelastic interaction: $\psi=\psi_0+0.3z\,\mathrm{sech}(z)$. ψ_0 represents an unperturbed sine-Gordon soliton.

$$u_k=\mp\frac{i}{4}\sqrt{2\pi}\frac{B^2\beta^2\gamma'^2}{\beta^2-\beta_t^2}\frac{1}{\omega_k}\mathrm{sech}\frac{k\pi}{2}\ . \tag{4.6}$$

The continuum contribution to $\zeta(z)$ is, according to Eq. (2.26b),

$$\zeta_c(z)=\int_{-\infty}^{\infty}dk\,u_k f_k(z)=\mp\frac{B^2\beta^2\gamma'^2}{\beta^2-\beta_t^2}\frac{z}{2}\mathrm{sech}(z)\ . \tag{4.7}$$

Therefore, the domain-wall's profile suffers modification in the presence of magnetoelastic coupling. This is shown in Fig. 6. Domain-wall modification $\zeta_c(z)$ can be large if β approaches β_t. In this case, higher-order consideration is required.

V. CONCLUSION

We have established a soliton perturbation theory for realistic domain-wall dynamics through the use of effective-field theory. The soliton perturbation scheme is most appropriate for materials of high-saturation magnetiza- tion and is therefore complementary to the perturbation scheme developed by Slonczewdki, which is appropriate for materials of low-saturation magnetization. While there are three different domain-wall configurations existing in Slonczewski's perturbation scheme, the soliton profile of a domain wall is stable against any (internal) perturbation in the present soliton perturbation scheme.

When the motion of a domain wall is considered under the influence of a static field and Gilbert damping, the soliton perturbation results coincide with Walker's solution up to the second perturbation order. This provides a support for the assumption admitting Walker's solution. Magnetoelastic interaction has also been considered as a perturbation to domain-wall motion. We found that magnetoelastic interaction modifies the wall's profile without changing its velocity in lowest order. Local dynamic strains can also be induced through the motion of the wall via magnetoelastic interaction. Dynamic strains are usually small except at resonance where the wall moves with a velocity equal to the transverse sound velocity. In this situation the wall will drag a large amount of elastic distortion along with it and, as in the case of anomalous microwave transmission, this might cause anomalous domain-wall velocity or penetration. For most magnetic materials the virtual magnon velocity c_0 and the transverse sound velocity c_t are roughly of the same order. Therefore, depending on the temperature and (dopant) composition, it is desirable to choose a material in which $c_0 \gg c_t$ such that the domain-wall velocity resonance can be achieved. This is most likely to happen for a material which is magnetically stiff (high Curie temperature) but mechanically soft (low Debye temperature). Finally, we note here that, due to the linearity of the soliton perturbation theory, Eqs. (2.16a) and (2.16b), the results concerning applied field and Gilbert damping derived in Sec. III are additive with those for magnetoelastic interaction derived in Sec. IV.

ACKNOWLEDGMENTS

This work was supported by Army Research Office (ARO) Contract No. DAAG29-84-K-0056.

*Present address: Department of Electrical and Computer Engineering, Northeastern University, Boston, MA 02115.

[1]M. B. Fogel, S. E. Trullinger, A. R. Bishop, and J. A. Krumhansl, Phys. Rev. B **15**, 1578 (1977).
[2]M. B. Fogel, S. E. Trullinger, and A. R. Bishop, Phys. Lett. **59A**, 81 (1976).
[3]D. I. Paul, J. Appl. Phys. **50**, 2128 (1979).
[4]U. Enz, Helv. Phys. Acta. **37**, 245 (1964).
[5]A. I. Akhiezer, V. G. Bar'Yakhtar, and M. I. Kaganov, Usp. Fiz. Nauk **3**, 781 (1961) [Sov. Phys.–Usp. **3**, 567 (1961)].
[6]F. R. Morgenthaler, IEEE Trans. Magn. **MAG-8**, 130 (1972).
[7]C. Kittel, Phys. Rev. **80**, 918 (1950).
[8]R. W. DeBlois, J. Appl. Phys. **29**, 459 (1958).
[9]L. Walker, analysis presented by J. R. Dillon, Jr., in *Magnetism*, edited by G. T. Rado and H. Suhl (Academic, New York, 1963), Vol. III, pp. 450–453.
[10]R. K. Dodd, J. C. Eilbeck, J. D. Gibbon, and H. C. Morris, *Solitons and Nonlinear Wave Equations* (Academic, New York, 1982), p. 437.
[11]C. Kittel, Phy. Rev. **110**, 836 (1958).
[12]D. E. Eastman, Phys. Rev. **82**, 715 (1966).
[13]J. W. Winter, Phys. Rev. **124**, 452 (1961).
[14]J. R. Slonczewski, Int. J. Magn. **2**, 85 (1972).
[15]R. C. O'Handley, J. Appl. Phys. **46**, 4996 (1975), and Refs. 8

and 11 therein.
[16]J. F. Currie, J. A. Krumhansl, A. R. Bishop, and S. E. Trumllinger, Phys. Rev. B **22**, 477 (1980).
[17]J. F. Currie, Phys. Rev. A **16**, 1692 (1977).
[18]B. Heinrich, J. F. Cochran, and K. Myrtle, J. Appl. Phys. **53**, 2090 (1982).
[19]G. C. Alexandrakis, R. A. B. Devin, and J. H. Abeles, J. Appl. Phys. **53**, 2095 (1982).